Neuron 49, 845–860, March 16, 2006 ©2006 Elsevier Inc. DOI 10.1016/j.neuron.2006.02.025

Targeted In Vivo Mutations of the AMPA Receptor Subunit GluR2 and Its Interacting Protein PICK1 Eliminate Cerebellar Long-Term Depression

Jordan P. Steinberg,[1,2,5] Kogo Takamiya,[1,2,5] Ying Shen,[2] Jun Xia,[3] Maria E. Rubio,[4] Sandy Yu,[1,2] Wenying Jin,[3] Gareth M. Thomas,[1,2] David J. Linden,[2] and Richard L. Huganir[1,2,*]

[1] Howard Hughes Medical Institute and
[2] Department of Neuroscience
Johns Hopkins School of Medicine
Baltimore, Maryland 21205
[3] Department of Biochemistry
Hong Kong University of Science and Technology
Clear Water Bay, Kowloon
Hong Kong
China
[4] Departments of Physiology and Neurobiology
University of Connecticut
Storrs, Connecticut 06269

Summary

Cerebellar long-term depression (LTD) is a major form of synaptic plasticity that is thought to be critical for certain types of motor learning. Phosphorylation of the AMPA receptor subunit GluR2 on serine-880 as well as interaction of GluR2 with PICK1 have been suggested to contribute to the endocytic removal of postsynaptic AMPA receptors during LTD. Here, we show that targeted mutation of PICK1, the GluR2 C-terminal PDZ ligand, or the GluR2 PKC phosphorylation site eliminates cerebellar LTD in mice. LTD can be rescued in cerebellar cultures from mice lacking PICK1 by transfection of wild-type PICK1 but not by a PDZ mutant or a BAR domain mutant deficient in lipid binding, indicating the importance of these domains in PICK1 function. These results demonstrate that PICK1-GluR2 PDZ-based interactions and GluR2 phosphorylation are required for LTD expression in the cerebellum.

Introduction

Cerebellar LTD is a persistent attenuation of synaptic strength at the parallel fiber-Purkinje cell synapse that results from repeated coactivation of parallel fiber and climbing fiber inputs to a Purkinje cell. It is widely thought to underlie various forms of motor learning such as associative eyelid conditioning and adaptation of the vestibulo-ocular reflex (Bear and Linden, 2000; Boyden et al., 2004). Previous work has shown that cerebellar LTD is induced by simultaneous activation of ionotropic AMPA receptors and metabotropic mGluR1 receptors as well as voltage-gated calcium channels on postsynaptic Purkinje cell terminals (Bear and Linden, 2000; Ito, 2002). The resultant rise in postsynaptic Ca^{2+} and liberation of diacylglycerol activates PKCα, which phosphorylates AMPA receptors on the GluR2 subunit and promotes the removal of AMPA receptors via clathrin-mediated endocytosis (Chung et al., 2003; Leitges et al., 2004; Linden, 2001; Matsuda et al., 2000; Wang and Linden, 2000). Results from rescue experiments performed in GluR2 knockout Purkinje cell cultures support this mechanism by showing GluR2 serine-880 (S880) to be the critical PKCα substrate for cerebellar LTD expression (Chung et al., 2003).

The Protein Interacting with C-Kinase 1 (PICK1) is a 55 kDa cytosolic protein with a single PDZ domain (Staudinger et al., 1995, 1997). The PDZ domain of PICK1 is unusual in that it can bind both type I and type II PDZ ligands. PKCα, the first identified ligand (Staudinger et al., 1997), has a carboxy-terminal sequence (QSAV) matching the consensus for a type I interaction (Songyang et al., 1997). The PICK1-PKCα interaction appears to be important for cerebellar LTD expression, potentially by serving to recruit PKCα to its proper subcellular target for phosphorylation (Leitges et al., 2004). GluR2, the critical PKCα target for cerebellar LTD, also binds directly to PICK1 (Dev et al., 1999; Xia et al., 1999), but through a type II PDZ interaction (Songyang et al., 1997). Interestingly, S880 of GluR2 lies within the type II PDZ ligand (S880-VKI) and, consequently, implicates phosphorylation in the dynamic regulation of GluR2 interactions during plasticity (Chung et al., 2000; Matsuda et al., 1999). Previous work has shown that S880 phosphorylation disrupts GluR2 binding to the PDZ domain containing protein GRIP1/2 but does not affect binding to PICK1 (Chung et al., 2000; Matsuda et al., 1999). It has thus been proposed that upon activation of PKCα and phosphorylation of GluR2, GRIP1/2 binding is disrupted, PICK1 binding is favored, and AMPA receptor endocytosis is facilitated. Studies involving the perfusion of PDZ domain interfering peptides or antibodies into cultured Purkinje cells support the importance of the PICK1-GluR2 interaction in cerebellar LTD expression. When a phoshoS880-VKI peptide or PICK1 PDZ domain-directed antibody designed to specifically interfere with the binding of PICK1 to GluR2 was introduced into Purkinje cells, a large attenuation of subsequent LTD induction was observed (Xia et al., 2000).

The recent finding that PICK1 belongs to a large family of proteins containing a BAR (Bin/amphiphysin/Rvs) domain (Habermann, 2004; Peter et al., 2004) supports a direct role for PICK1 in endocytosis. Present in a number of small GTPase binding and endocytic pathway proteins, BAR domains exist as dimers of coiled-coil domains that come together in a banana-shaped crescent. The tips of the crescent contain clusters of positively charged lysine residues that appear to mediate binding to negatively charged phospholipids. By either sensing areas of preferred membrane curvature or actively bending the membrane for subsequent budding, BAR domains are believed to facilitate endocytosis (Peter et al., 2004). Subsequent to binding GluR2, PICK1 dimers may localize AMPA receptor complexes to lateral margins of the postsynaptic density where endocytosis is thought to occur (Blanpied et al., 2002; Racz et al., 2004).

In this study, we first focused on the role of the PICK1-GluR2 interaction in cerebellar LTD through a reciprocal

*Correspondence: rhuganir@jhmi.edu
[5] These authors contributed equally to this work.

strategy of genetic deletion. We generated homozygous knockout (KO) mice lacking PICK1 (PICK1 KO) as well as homozygous knockin (KI) mice with a mutant form of the GluR2 AMPA receptor subunit lacking the last seven amino acids (GluR2Δ7 KI). The GluR2Δ7 mutation eliminates the C-terminal type II PDZ ligand and disrupts the interaction of GluR2 with PICK1 and GRIP1/2. Second, we generated KI mice containing a mutant form of GluR2 designed to prevent PKCα-mediated phosphorylation at S880 (GluR2 K882A KI). This mouse line incorporates a lysine mutation in the consensus recognition motif for PKC (S/T-X-K/R) (Kemp and Pearson, 1990) and thereby prevents phosphorylation of S880. The mutant mouse lines were subject to anatomical and biochemical characterization as well as electrophysiological analysis in both cerebellar cultures and brain slices. Together, our studies indicate a clear in vivo requirement for PDZ-dependent interactions between PICK1 and GluR2, as well as phosphorylation of GluR2 at S880, in the expression of cerebellar LTD.

Results

PICK1 KO and GluR2Δ7 KI Mice Have Normal Levels of AMPA Receptors but Altered GluR2 Ultrastructural Localization

PICK1 KO and GluR2Δ7 KI mice were generated by homologous recombination as described previously (Gardner et al., 2005). Homozygous mice derived from both lines were viable and showed no gross developmental defects. No obvious abnormalities in cerebellar architecture or defects in Purkinje cell dendritic elaboration were observed in Nissl- and Golgi-stained brain sections, respectively (Figure S1).

The levels of AMPA receptor subunits and associated proteins in PICK1 KO (Figure 1A) and GluR2Δ7 KI mice (Figure 1B) were determined by Western blotting of cerebellar and hippocampal tissue samples from 3–4 week old animals. The absence of PICK1 protein in PICK1 KO mice was confirmed with several antibodies to PICK1 directed against both N- and C-terminal regions (Figure 1A and data not shown). The expression levels of all four major AMPA receptor subunits (GluR1–GluR4), measured by using a variety of subunit-specific antibodies, were equal among PICK1 KO mice and wild-type (wt) littermates. In addition, the levels of splice variants of GluR2 and GluR4 (GluR2L and GluR4c) were similar in wt and PICK1 KO mice. In GluR2Δ7 KI mice, the absence of the C-terminal 7 amino acids (C-7) of GluR2 was confirmed with an antibody purified to recognize only the last seven amino acids. However, a GluR2 N-terminal antibody (which reacts with both GluR2 and GluR2L) showed equal levels in GluR2Δ7 KI mice and wt littermates. The expression levels of GluR1, GluR3, GluR4, and GluR4c were also similar between wt and GluR2Δ7 KI mice. A GluR2/3/4c C-terminal antibody showed a reduction in GluR2Δ7 KI mice but likely reflects loss of the strong GluR2 C-7 epitope rather than a reduction in GluR2 levels because this difference was nearly eliminated by preabsorbing the antibody with C-7 peptide. Unexpectedly, levels of GluR2L, which does not contain a known PDZ ligand, were elevated approximately 5-fold in GluR2Δ7 KI samples from both cerebellum and hippocampus. Although care was taken to preserve the 3′ splice site during generation of the GluR2Δ7 KI line, the elevation in GluR2L levels suggests altered regulation of splicing in these mice. Nonetheless, we believe GluR2L to be only a very minor contributor to total GluR2 levels based on two findings. First, as mentioned above, total levels of GluR2 detected with a GluR2 N-terminal antibody were equal among GluR2Δ7 KI mice and wt littermates. Second, immunodepletion of GluR2L from 3–4 week old wt brain samples resulted in no apparent decrease of total GluR2 levels detected with a GluR2 N-terminal antibody, whereas immunodepletion of GluR2 (short form) resulted in complete elimination of the total GluR2-N signal (Figure S2).

To confirm our Western blot findings, we performed immunoperoxidase staining in cerebellar sections of 3–4 week old PICK1 KO (Figure 1C) and GluR2Δ7 KI mice (Figure 1D). Antibodies to PICK1 and GluR2 C-7 confirmed absence of these two epitopes as seen in Western blots. In PICK1 KO mice, GluR2 staining (either with GluR2 C-7 or GluR2/3/4c antibodies) was comparable to that in wt littermates. In GluR2Δ7 KI mice, a reduction in GluR2/3/4c staining attributable to loss of the GluR2 C-7 epitope was again seen. This difference was nearly eliminated by preabsorbing the antibody with the C-7 peptide (data not shown). GluR1, expressed predominantly in Bergmann glial processes rather than Purkinje cells at this age (Baude et al., 1994), stained similarly in wt and homozygous mice of both mutant lines.

Recent studies have suggested that the interaction between PICK1 and PKCα subserves a key role in targeting PKCα to GluR2 during synaptic plasticity (Leitges et al., 2004; Lu and Ziff, 2005; Perez et al., 2001). To determine the effect of PICK1 deletion on GluR2 S880 phosphorylation, we used a S880 phospho-specific antibody (Chung et al., 2000) to analyze wt and PICK1 KO lysates prepared from high-density cortical neurons treated with the PKC-activating phorbol-12-myristate-13-acetate (TPA, 200 nM) or with media containing an equal volume of DMSO as a control (Figure 1E). As observed previously in rat cultures (Chung et al., 2000; Lu and Ziff, 2005; Perez et al., 2001), neurons derived from wt mice showed a robust increase in GluR2 S880 phosphorylation after 20 min of TPA stimulation relative to DMSO-treated controls ($p < 0.001$). Notably, we observed a similar TPA-induced increase in S880 phosphorylation in PICK1 KO neurons ($p < 0.001$). Moreover, basal phosphorylation was slightly higher in PICK1 KO neurons compared to neurons from wt littermates ($p < 0.05$). These results suggest that PICK1 is not required on a global level for PKC-mediated phosphorylation of GluR2 S880. Nonetheless, we cannot rule out the possibility that PICK1 may be important in recruiting PKCα to GluR2 at synapses because these receptors may constitute a small, biochemically undetectable pool of GluR2.

To examine the ultrastructural distribution of GluR2 at parallel fiber-Purkinje cell synapses in PICK1 KO and GluR2Δ7 KI mice, we performed immunoelectron microscopy on 3–4 week old mouse cerebella with a GluR2 N-terminal antibody. In wt littermates from both PICK1 (Figure 2) and GluR2Δ7 (Figure 3) mutant lines, GluR2 labeling was concentrated along the PSD with occasional gold particles located intracellularly within spines or at extrasynaptic plasma membrane regions. The degree of PSD labeling was unchanged in PICK1 KO mice

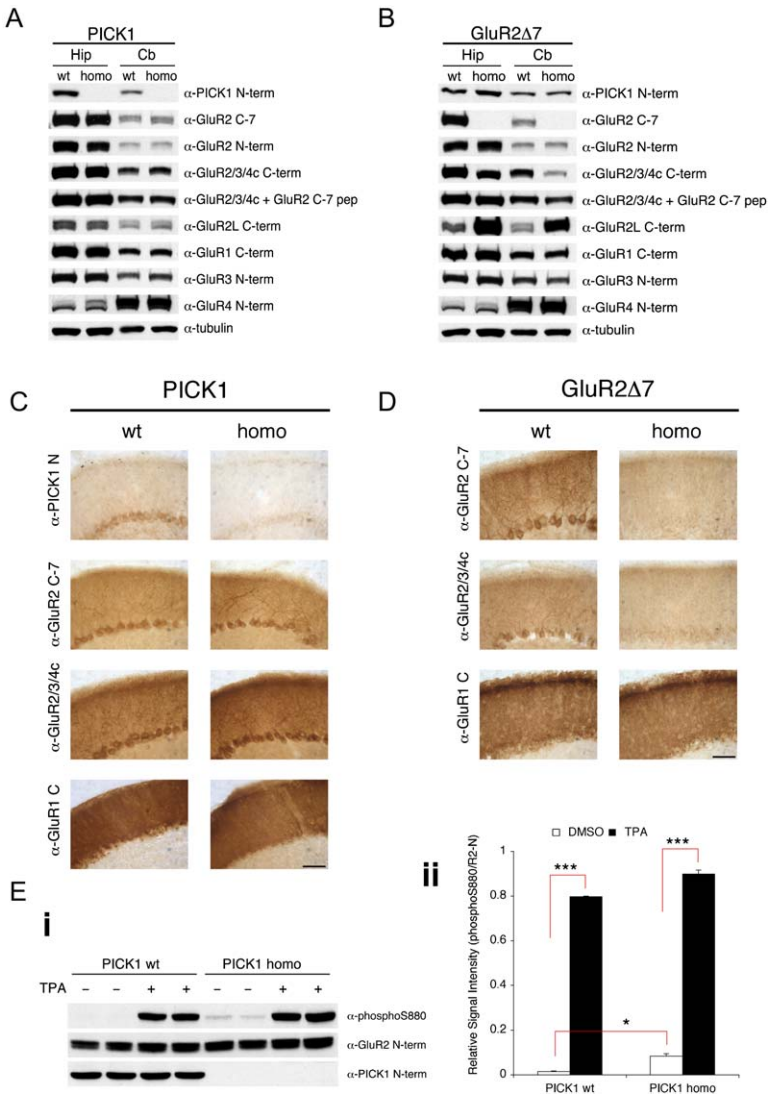

Figure 1. Biochemical and Immunohistochemical Characterization of PICK1 KO and GluR2Δ7 KI Mice

(A) Western blot of hippocampal (Hip) and cerebellar (Cb) homogenates from 3–4 week old PICK1 KO (homo) mice and wt littermates. α-GluR2 C-7 denotes an antibody specific for the C-terminal 7 amino acids of GluR2. GluR2 C-7 pep represents the corresponding GluR2 C-terminal 7 amino acid peptide used for purification of this antibody.

(B) Western blot from 3–4 week old GluR2Δ7 KI (homo) mice and wt littermates.

(C) Immunoperoxidase staining in 3–4 week old PICK1 KO mice and wt littermates. Scale bar = 100 μm.

(D) Immunoperoxidase staining in 3–4 week old GluR2Δ7 KI mice and wt littermates. Scale bar = 100 μm.

(E) Phorbol ester stimulation in high-density cortical neuron cultures from PICK1 KO mice and wt littermates. (Ei) 10 day old cortical neurons were treated in duplicate with 200 nM TPA for 20 min (or DMSO as a control), lysed, and analyzed by Western blot with a phospho-specific S880 antibody (Chung et al., 2000). (Eii) S880 phosphorylation signal intensities relative to total GluR2-N signal intensities were quantified for each lane and averaged. Error bars = SEM. Asterisk, $p < 0.05$; triple asterisk, $p < 0.001$.

(11.50 ± 1.80 [mean ± SEM] versus 11.60 ± 1.72 gold particles/μm PSD for wt) and in GluR2Δ7 KI mice (9.85 ± 1.73 versus 10.40 ± 2.45 gold particles/μm PSD for wt). Interestingly, the degree of extrasynaptic plasma membrane GluR2 labeling in spines of both PICK1 KO (1.84 ± 0.32 versus 1.00 ± 0.22 gold particles/μm for wt, $p < 0.05$) and GluR2Δ7 KI mice (2.24 ± 0.36 versus 0.39 ± 0.20 gold particles/μm for wt, $p < 0.05$) was significantly increased. Moreover, the degree of intracellular GluR2 labeling was higher within spines of PICK1 KO (34.80 ± 4.92 versus 14.52 ± 3.45 gold particles/μm^2 for wt, $p < 0.001$) and GluR2Δ7 KI mice (30.25 ± 6.09 versus 8.57 ± 4.95 gold particles/μm^2 for wt, $p < 0.001$). These increases in spine GluR2 labeling were concomitant with a significant decrease in the degree of intracellular GluR2 labeling within dendrites and cell bodies of both PICK1 KO (18.80 ± 2.77 versus 31.66 ± 2.16 gold particles/μm^2 for wt, $p < 0.001$) and GluR2Δ7 KI mice (4.43 ± 0.72 versus 26.70 ± 5.10 gold particles/μm^2 for wt, $p < 0.001$). Taken together with the Western blot data showing equal total levels of GluR2 among wt and homozygous mice of each mutant line, these results suggest a redistribution of GluR2-containing AMPA receptors from somatic and dendritic compartments to extrasynaptic regions of spines in PICK1 KO and GluR2Δ7 KI mice. Although equal PSD labeling suggests the maintenance of a normal steady-state synaptic GluR2 pool in homozygous mice, the accumulation of GluR2 at extrasynaptic plasma membrane regions and intracellularly within Purkinje cell spines suggests aberrant trafficking into and out of the synaptic compartment.

Cerebellar LTD Is Absent in PICK1 KO Mice

To test the hypothesis that cerebellar LTD expression requires PICK1, we first measured LTD in dissociated cerebellar cultures derived from PICK1 KO mice. Purkinje cells were held at −70 mV, and test pulses of glutamate (30–90 ms long, delivered at 0.05 Hz) evoked an AMPA-receptor mediated inward current that was stable during the baseline recording period (Figure 4A). When wt Purkinje cells received induction stimuli consisting of six 3 s long depolarizations to 0 mV, each paired with a pulse of glutamate, an immediate and persistent depression resulted in response to subsequent test pulses (50% ± 8.3% of baseline [mean ± SEM], t = 17.5 min, n = 8). This LTD was maximal because later

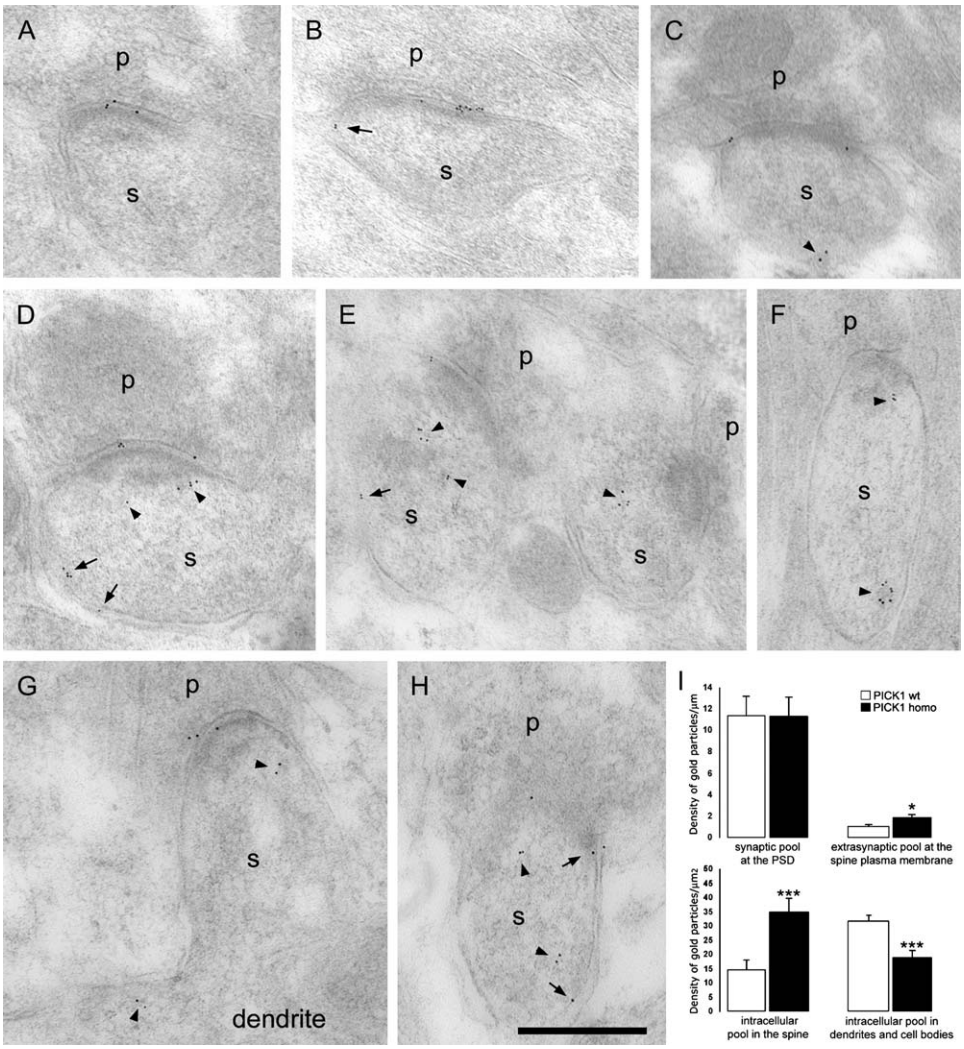

Figure 2. Immunoelectron Microscopy Reveals Altered GluR2 Ultrastructural Localization in PICK1 KO Mice

(A–C) Immunogold labeling using a GluR2 N-terminal antibody in wt littermates. Gold particles are preferentially observed at the PSD of parallel fiber-Purkinje cell synapses. Rare labeling at the plasma membrane (arrows) or intracellularly within spines (arrowheads) can be seen. (s = Purkinje cell dendritic spine; p = parallel fiber synapses.)

(D–H) In PICK1 KO (homo) mice, gold particles are also observed at the PSD. Additionally, numerous gold particles are localized extrasynaptically at the plasma membrane of Purkinje cell dendritic spines (arrows) and associated with smooth membranes of the endoplasmic reticulum (arrowheads) in spines. (s = Purkinje cell dendritic spine; p = parallel fiber synapses.)

(I) Quantitative analysis of immunogold labeling. Histograms show the density/μm of gold particles along the PSD and extrasynaptic spine plasma membrane (upper row) and intracellular density/μm^2 within the spine and in dendrites/cell bodies (lower row). Error bars = SEM. Asterisk, $p < 0.05$; triple asterisk, $p < 0.001$. s = Purkinje cell dendritic spine; p = parallel fiber synapses; scale bar = 0.2 μm.

induction stimuli consisting of 12 pairings induced no further depression (51% ± 7.1% of baseline, t = 40 min). In contrast, when pairing stimulation was delivered to PICK1 KO Purkinje cells, no LTD was observed and a mild potentiation was revealed (108% ± 7.8% of baseline at t = 17.5 min and 112% ± 9.0% of baseline at t = 40 min, n = 7). Mutant Purkinje cells displayed normal R_{input} as well as normal mEPSC amplitude and kinetics (Table S1). It is also unlikely that PICK1 deletion blocked LTD by disrupting essential initial transmembrane signals required for induction because microfluorimetric Ca^{2+} imaging revealed normal Ca^{2+} transients evoked by either depolarization or DHPG-evoked mGluR1 activation (Table S1).

To address the possibility that these results with PICK1 KO mice were restricted to cell culture, we repeated LTD experiments with acute parasagittal slices prepared from P20–P25 mice. Parallel fiber EPSCs were evoked by brief (100 μs) shocks delivered to the molecular layer, and Purkinje cells were whole-cell voltage clamped at a command potential of −70 mV. After a 20 min baseline recording period, parallel fibers were stimulated with a train of five pulses at 100 Hz, which was accompanied by a 100 ms long depolarization of the Purkinje cell to 0 mV. These bursts were repeated 30 times with an interburst interval of 2 s. Slices from wt littermates showed robust LTD (73% ± 3.0% of baseline at t = 40 min, n = 6), whereas those from

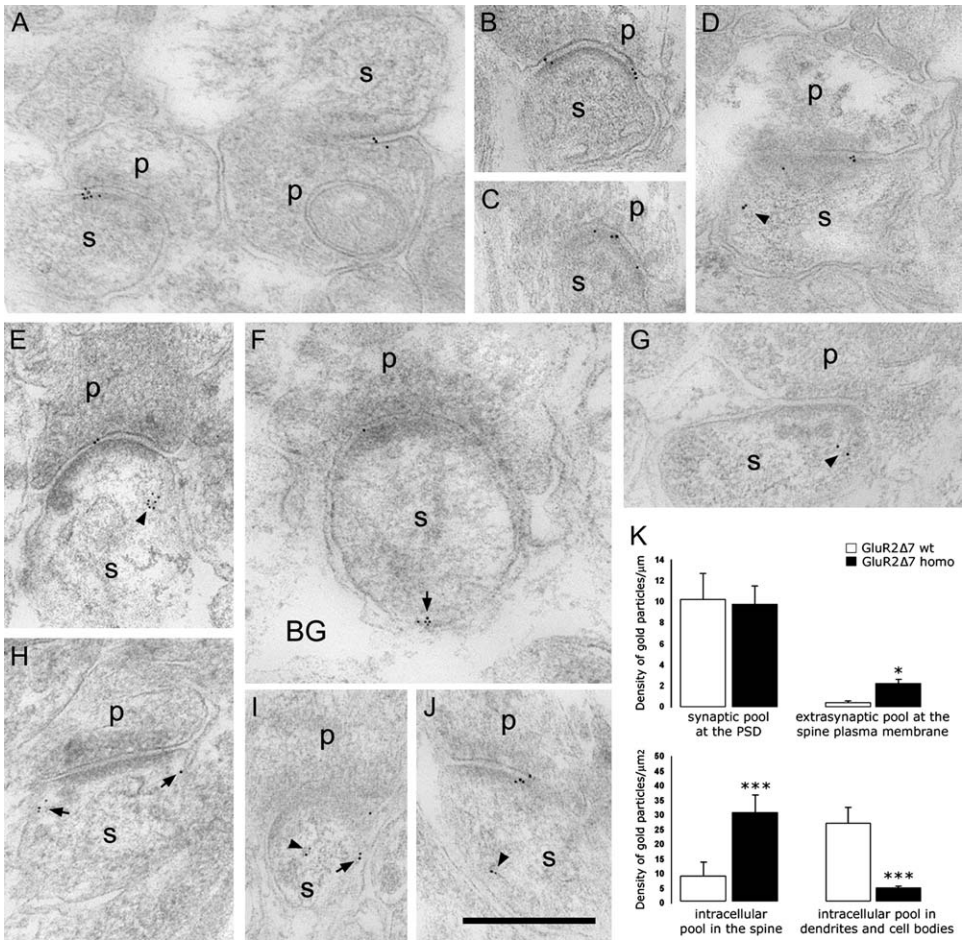

Figure 3. Immunoelectron Microscopy Reveals Similarly Aberrant GluR2 Localization in GluR2Δ7 KI Mice

(A–D) Gold particles in wt littermates are preferentially observed at the PSD of parallel fiber-Purkinje cell synapses with only occasional labeling at the extrasynaptic plasma membrane or intracellularly within spines (arrowheads). (s = Purkinje cell dendritic spine; p = parallel fiber synapses.) (E–J) Gold particles in GluR2Δ7 KI (homo) mice are observed at the PSD but also found in significant numbers at the extrasynaptic plasma membrane (arrows) and within the spine intracellular compartment (arrowheads). (s = Purkinje cell dendritic spine; p = parallel fiber synapses.) (K) Quantitative analysis of immunogold labeling. Histograms show the density/μm of gold particles along the PSD and extrasynaptic spine plasma membrane (upper row) and intracellular density/μm^2 within the spine and in dendrites/cell bodies (lower row). Error bars = SEM. Asterisk, $p < 0.05$; triple asterisk, $p < 0.001$. s = Purkinje cell dendritic spine; p = parallel fiber synapses; scale bar = 0.2 μm.

PICK1 KO mice did not (100% ± 3.6% of baseline at t = 40 min, n = 6) (Figure 4C).

PICK1 PDZ Domain Function Is Required for Cerebellar LTD

To examine the structural domains of PICK1 that are critical for LTD expression, we attempted to rescue LTD in PICK1 KO Purkinje cell cultures by gene gun-mediated transfection with wt and mutant PICK1 cDNA constructs. Purkinje cells transfected with a wt PICK1 construct showed a complete rescue of LTD (52% ± 7.8% of baseline at t = 17.5 min and 52% ± 6.8% of baseline at t = 40 min, n = 9) (Figure 4A). In contrast, a PICK1 cDNA construct with a mutation in the PDZ domain (K27A/D28A) (Staudinger et al., 1997; Xia et al., 1999) completely failed to rescue LTD (114% ± 8.0% of baseline at t = 17.5 min and 119% ± 8.4% of baseline at t = 40 min, n = 6) (Figure 4A). These results rule out a chronic, developmental effect of PICK1 deletion on the ability to induce cerebellar LTD and confirm the critical role of the PDZ domain in PICK1 function during LTD expression.

LTD that is both induced and monitored by glutamate test pulses has the advantage that it bypasses presynaptic events and allows for an analysis of postsynaptic mechanisms in isolation. One disadvantage, however, is that it measures both synaptic and extrasynaptic receptors. To determine whether PICK1 is required for cerebellar LTD specifically at synaptic AMPA receptors, we measured miniature excitatory postsynaptic currents (mEPSCs) and induced LTD chemically by a 10 min long bath application of the PKC activator phorbol-12,13-diacetate (PDA, 200 nM) (Figure 4B). As previously described (Chung et al., 2003; Linden and Connor, 1991), PDA produced an LTD-like effect appearing as a slowly developing, but ultimately stable, decrease in the mean amplitude of mEPSCs (from 33 ± 4.1 pA at t = −10 min to 15 ± 5.8 pA at t = 35 min, n = 10). Analysis of the LTD-like phenomenon produced by PDA showed that it generally followed the results with glutamate/depolarization

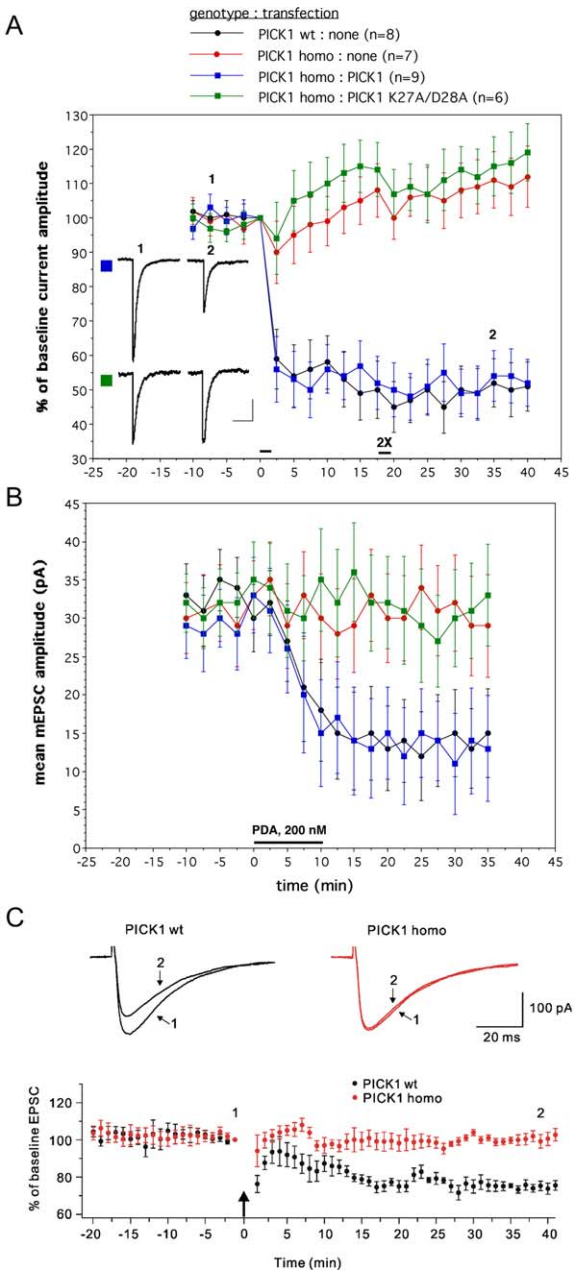

Figure 4. Cerebellar LTD Is Abolished in Cultures and Acute Slices from PICK1 KO Mice and Cannot Be Rescued by a PDZ Domain Mutant of PICK1

(A) After baseline recording of glutamate-evoked inward currents, LTD was induced in cultures by iontophoretic glutamate pulses in conjunction with depolarization. Six pairings were delivered at t = 0 min (horizontal bar) and 12 pairings at t = 17.5 min (horizontal bar, 2×). Representative single current traces were acquired at the indicated times. Scale bars = 1 s, 50 pA. PICK1 KO cultures were either untransfected, transfected with wt PICK1, or transfected with the PICK1 K27A/D28A PDZ domain mutant.

(B) An LTD-like effect was induced in cultures by bath application of 200 nM PDA at t = 0–10 min as indicated by the horizontal bar. mEPSCs were measured and are expressed as mean raw amplitudes (rather than a normalized scale). n = 10 cells/group.

(C) After baseline acquisition of parallel fiber EPSCs, LTD was induced in cerebellar slices by pairing brief parallel fiber bursts with depolarization as indicated by the arrow at t = 0 min. Representative current traces are the average of three consecutive responses, taken at the times indicated on the graph. n = 6 cells/group. It should be noted that, in slices, LTD is typically slower to develop after conditioning stimulation and is of smaller amplitude compared to that seen in cultures. Error bars = SEM for all graphs.

pairing: PICK1 KO Purkinje cells showed no depression (from 30 ± 4.6 pA at t = −10 min to 29 ± 6.7 pA at t = 35 min, n = 10) that could be rescued by transfection with wt PICK1 (from 29 ± 4.3 pA at t = −10 min to 13 ± 6.9 pA at t = 35 min, n = 10) but not by the K27A/D28A PDZ mutant of PICK1 (from 32 ± 3.8 pA at t = −10 min to 33 ± 6.6 pA at t = 35 min, n = 10). These results indicate that PICK1 PDZ domain function is required for the depression of synaptic AMPA receptor currents and that PICK1 deletion is unlikely to block LTD induction through effects on processes prior to PKCα activation.

PICK1 BAR Domain Function Is Required for Cerebellar LTD

Recent homology studies have indicated that in addition to its N-terminal PDZ domain, PICK1 contains a BAR domain (Peter et al., 2004). BAR domain proteins comprise a large family of GTPase binding and endocytic pathway proteins including arfaptin2 and amphiphysin, respectively (Habermann, 2004). Recent crystallization of the BAR domains in these two proteins has revealed critical residues mediating association with lipid bilayers for sensing and/or induction of membrane curvature. These positively charged lysine and arginine residues are found at the tips of the banana-shaped BAR domain dimer structure (Peter et al., 2004) (Figure 5A).

To investigate the function of the putative BAR domain in PICK1 and its potential involvement in cerebellar LTD, we attempted to rescue LTD in PICK1 KO Purkinje cell cultures by using cDNA constructs with targeted mutations in the BAR domain. In one construct, lysines at positions 266 and 268 within the loop region were mutated to glutamates (K266E/K268E) to attenuate lipid association (Figure 5A). Selection of these residues was based on previously characterized mutations in amphiphysin at the corresponding region that blocked association with lipids and membrane tubulation in vitro (Peter et al., 2004). In the second construct, a cluster of leucines toward the interior of the first helix and away from the positively charged loop region were mutated to glutamates (L149E/L156E/L162E) (Figure 5A). We tested the ability of each mutant to coprecipitate with phospholipid extracts by a method previously described for amphiphysin (Peter et al., 2004). Equal amounts of purified PICK1 protein were incubated with phospholipid mixtures for 15 min at 37ºC and centrifuged. Pellets and supernatants were then analyzed independently by SDS-PAGE. Comparable to wt PICK1, a significant fraction of the L149E/L156E/L162E helix-region mutant copelleted with lipids (Figure 5B). However, the K266E/K268E loop-region mutant showed a marked reduction in lipid binding capability (Figure 5B) ($p < 0.05$) consistent with structural predictions.

In PICK1 KO Purkinje cells transfected with a PICK1 K266E/K268E mutant cDNA construct, LTD evoked by glutamate/depolarization pairing was completely blocked (107% ± 9.0% of baseline at t = 40 min, n = 6) (Figure 5C). By contrast, LTD was largely rescued in L149E/L156E/L162E-transfected cultures (66% ± 7.8%

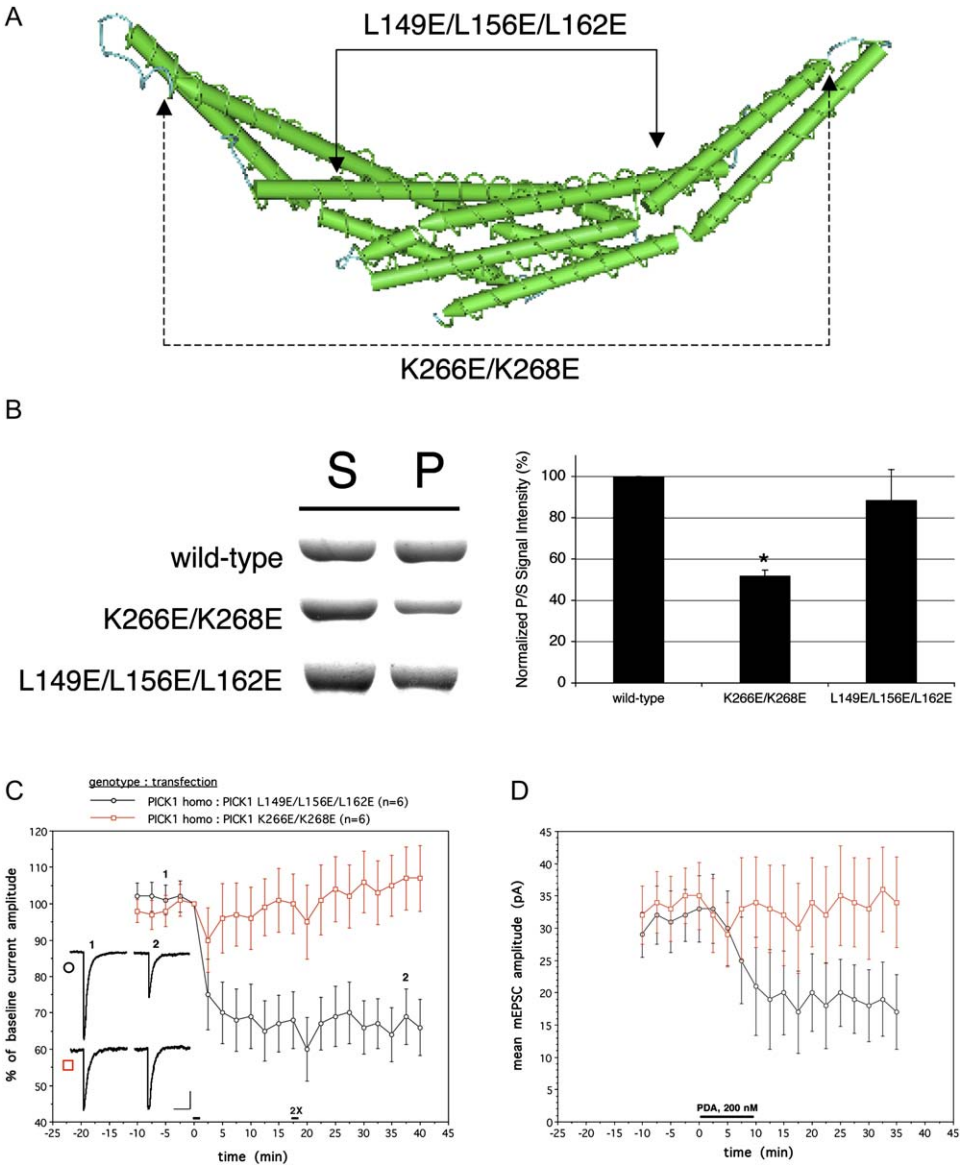

Figure 5. A Lipid-Binding-Deficient BAR Domain Mutant of PICK1 Fails to Rescue Cerebellar LTD in Cultures from PICK1 KO Mice

(A) Schematic representation of PICK1 BAR domain based on arfaptin2 crystal structure (Tarricone et al., 2001).

(B) In vitro lipid binding assay. (Bi) Equal amounts of PICK1 fusion protein were incubated with lipid extracts and centrifuged. S = supernatant; P = pellet. (Bii) Quantitative analysis of pellet-to-supernatant (P/S) signal intensity ratio (normalized to the P/S signal intensity ratio for wt). n = 6 experiments per construct. Error bars = SEM. Asterisk, $p < 0.05$.

(C) PICK1 KO Purkinje cells were transfected with the PICK1 K266E/K268E or PICK1 L149E/L156E/L162E BAR domain mutant. LTD induction was attempted with six pairings delivered at t = 0 min (horizontal bar) and 12 pairings at t = 17.5 min (horizontal bar, 2×). Scale bars = 1 s, 50 pA.

(D) An LTD-like effect on mEPSC amplitude was induced by bath application of PDA as indicated by the horizontal bar. n = 10 cells/group. Error bars = SEM for all graphs.

of baseline at t = 40 min, n = 6). A similar pattern was observed when PDA-evoked depression of mEPSCs was assessed: K266E/K268E-transfected cultures showed no depression from basal values (from 32 ± 4.5 pA at t = −10 min to 34 ± 7.0 pA at t = 35 min, n = 10), whereas L149E/L156E/L162E-transfected cultures showed typical depression (from 29 ± 3.5 pA at t = −10 min to 17 ± 5.8 pA at t = 35 min, n = 10) (Figure 5D). These results indicate a critical function for lysine residues in the loop region of the PICK1 BAR domain and suggest a key role for PICK1-mediated lipid binding in endocytosis events associated with cerebellar LTD. Nonetheless, we cannot rule out the possibility that the K266E/K268E mutation has an effect on some other functional property of PICK1.

Cerebellar LTD Is Absent in GluR2Δ7 KI Mice

Our studies of cerebellar LTD in preparations from PICK1 KO mice suggest a critical role for this PDZ domain-containing protein. However, since the PICK1 PDZ domain mediates binding to both PKCα and GluR2, our rescue studies in PICK1 KO Purkinje cell cultures with the K27A/D28A PDZ domain mutant of PICK1 do not distinguish between these two interactions. To focus

more specifically on the PICK1-GluR2 PDZ-dependent interaction, we analyzed LTD in dissociated cultures and acute parasagittal slices from GluR2Δ7 KI mice.

Pairing-evoked LTD monitored with glutamate pulses was normal in cultures derived from wt controls (53 ± 9.4% of baseline at t = 40 min, n = 7) but was completely blocked in cultures from GluR2Δ7 KI mice (120% ± 9.9% of baseline at t = 40 min, n = 7) (Figure 6A). Similarly, PDA treatment depressed mEPSC amplitude in cultures from wt littermates (from 33 ± 4.6 pA at t = −10 min to 16 ± 5.7 pA at t = 35 min, n = 10) but failed to do so in GluR2Δ7 KI cultures (from 31 ± 3.8 pA at t = −10 min to 36 ± 7.0 pA at t = 35 min, n = 10) (Figure 6B). Acute cerebellar slices from GluR2Δ7 KI mice also failed to show LTD (98% ± 3.1% of baseline at t = 40 min, n = 6), whereas slices from wt littermates revealed typical depression (76% ± 1.0% of baseline at t = 40 min, n = 6) (Figure 6C). These results in dissociated Purkinje cell cultures and acute slice preparations from GluR2Δ7 KI mice demonstrate a critical role for the GluR2 PDZ ligand in cerebellar LTD.

GluR2 K882A KI Mice Show Impaired PKC-Mediated Phosphorylation and Altered GluR2 Ultrastructural Localization

We have previously shown that mutation of K882 within the intracellular C terminus of the GluR2 subunit (GluR2 K882A) to ablate the S/T-X-K/R kinase recognition motif (Kemp and Pearson, 1990) prevents PKC-mediated phosphorylation at S880 (Chung et al., 2003). Furthermore, we have shown that the K882A mutation (at the −1 position of the C-terminal PDZ ligand) does not interfere with binding to the PDZ domain-containing proteins, PICK1 and GRIP1 (Chung et al., 2003; Seidenman et al., 2003). When a GluR2 cDNA construct containing this mutation was transfected into LTD-deficient GluR2 knock-out Purkinje cells in culture, no rescue was achieved (Chung et al., 2003). GluR2 phosphorylation at S880 therefore appears to be the key initial regulatory step modulating the removal of AMPA receptors from the cell surface during LTD. We generated GluR2 K882A KI mice with a similar strategy to that used for the GluR2Δ7 KI line as a specific test of this hypothesis (Figures 7A and 7B) (Gardner et al., 2005).

The GluR2 K882A KI mice were viable and were without any observable developmental defects. Cerebellar architecture and Purkinje cell morphology appeared grossly normal by Nissl and Golgi staining (Figure S1). Western blotting with GluR1, GluR2, GluR3, and GluR4 subunit-specific antibodies showed normal AMPA receptor levels in GluR2 K882A KI mice at 1 and 3 months of age in both cerebellum and hippocampus (Figure 7C). A reduction was seen with a GluR2 C-7 antibody but likely reflects disruption of the epitope by the K882A point mutation. Interestingly, a marked reduction in the levels of the GluR2L splice form was observed for GluR2 K882A KI mice relative to wt littermates in both brain regions, particularly at 1 month of age. This is in contrast to the distinct increase in GluR2L levels observed for GluR2Δ7 KI mice. As mentioned above, care was taken to preserve the 3′ splice site in the construction of both KI lines by introducing the most parsimonious base changes possible to produce the desired mutations. Despite this effort, it appears that inadvertent effects on

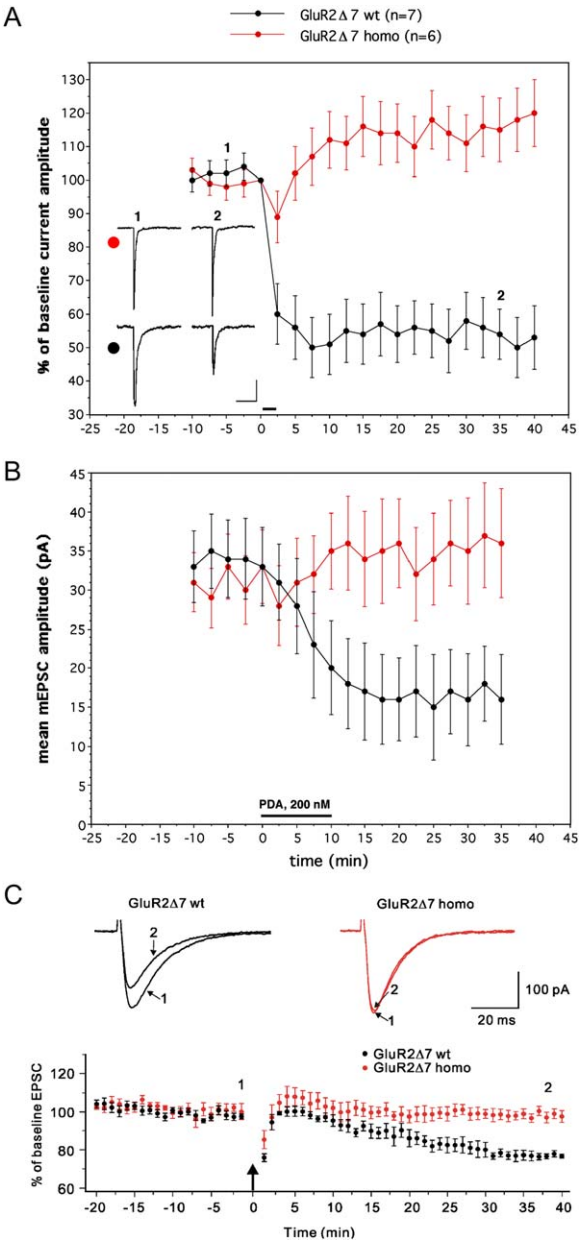

Figure 6. Cerebellar LTD Is Abolished in Cultures and Acute Slices from GluR2Δ7 KI Mice

(A) LTD was induced in cultures by six glutamate/depolarization pairings at t = 0 min. Scale bars for representative current traces = 1 s, 40 pA.

(B) An LTD-like effect on mEPSC amplitude was induced in cultures by bath application of PDA as indicated by the horizontal bar. n = 10 cells/group.

(C) Parallel fiber LTD in slices derived from GluR2Δ7 mice. n = 6 cells/group. Error bars = SEM for all graphs.

GluR2 splicing still occurred. Nonetheless, we believe this change in the level of GluR2L to be of negligible functional consequence because of the very small percentage of this splice form in 3–4 week old mouse brains (Figure S2).

To confirm the Western blot data, we analyzed immunohistochemical stains in sections of cerebellum from both wt and GluR2 K882A KI mice (Figure 7D). GluR2/3/4c staining in Purkinje cells was approximately equal

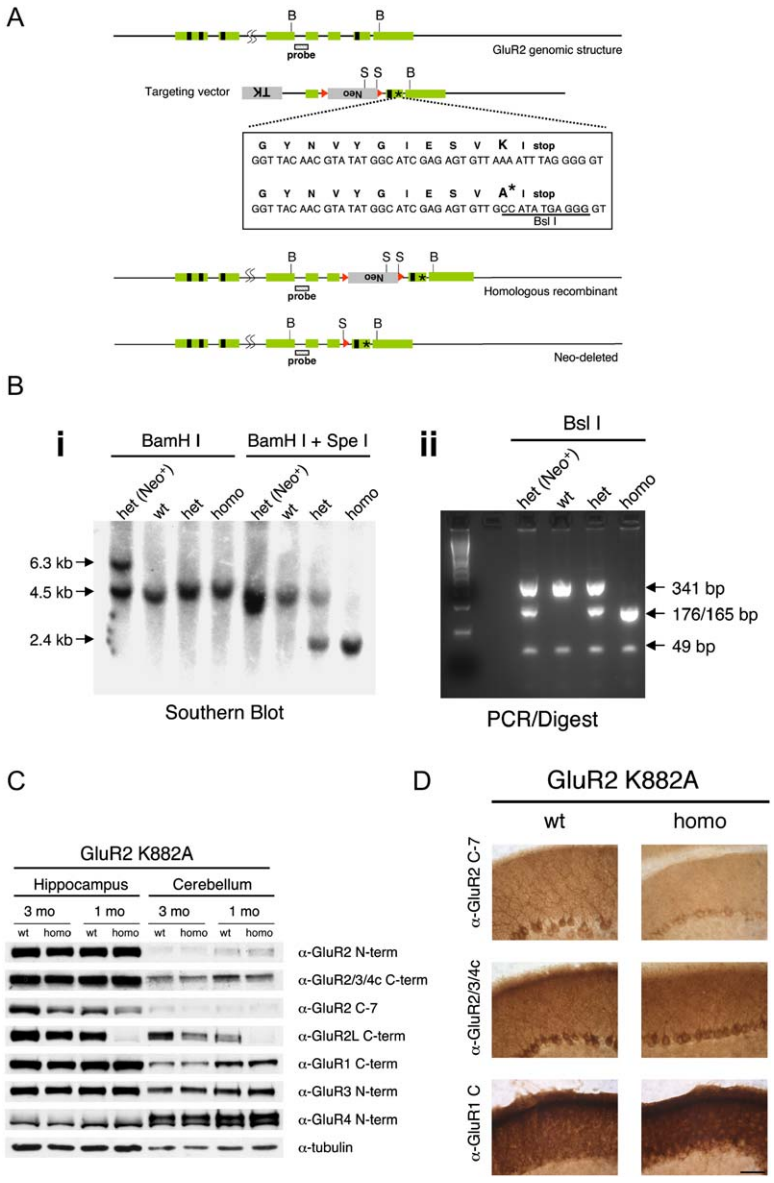

Figure 7. Genetic, Biochemical, and Immunohistochemical Characterization of GluR2 K882A KI Mice

(A) Schematic of KI targeting strategy. Genomic DNA structure of GluR2 3′ region is shown. Exons and transmembrane regions are indicated as green and black boxes, respectively. DNA and amino acid sequences are shown in detail in the box (top, wt, bottom, GluR2 K882A KI). The K882A mutation (asterisk), which also introduces a Bsl I site by conservative mutation of the surrounding codons, was generated by PCR. A Neo resistance cassette (Neo; gray box) with loxP sequences at both sides (red triangles) was introduced into the Bgl II site in the intron upstream of the exon containing transmembrane (TM) domain 4 and the C terminus region of GluR2. After germline transmission, Neo was deleted with the Cre/loxP system by breeding to CMV-Cre transgenic mice. B, BamH I sites; S, Spe I sites.

(B) Southern blot and PCR/restriction digest analysis of genomic DNA isolated from GluR2 K882A KI (homo) mice and wt littermates. (Bi) Southern blot was performed with an outer probe to the targeting vector as indicated in (A). BamH I digestion of wt genomic DNA generated a 4.5 kb fragment, whereas digestion of Neo$^+$ mutant genomic DNA produced a 6.3 kb fragment. After Neo deletion, fragments from each of the different genotypes were of indistinguishable size. Double enzyme digestion with BamH I and Spe I allowed separation of the mutant band because of an additionally introduced Spe I site from the loxP sequence (2.4 kb). (Bii) Genomic DNA was used as a PCR template to amplify a fragment surrounding the region of the GluR2 K882A mutation. These PCR products were then digested with Bsl I to confirm the presence of the mutation. Lane 2 shows Bsl I digestion of purified genomic DNA from a Neo$^+$ mouse. The 341 bp upper band represents amplification of the wt allele. The corresponding PCR product from the targeted allele was cleaved by Bsl I into two fragments of 176 and 165 bp, both of which run together as a single lower band. Only this single lower band is observed in homozygous DNA. An additional 49 bp Bsl I digest fragment is seen in all lanes.

(C) Western blot of hippocampal (Hip) and cerebellar (Cb) homogenates from 1 month old (mo) and 3 month old (mo) GluR2 K882A KI mice and wt littermates.

(D) Immunoperoxidase staining in 3–4 week old GluR2 K882A KI mice and wt littermates. Scale bar = 100 μm.

among wt and GluR2 K882A KI mice, whereas GluR2 C-7 staining was markedly reduced. The reduction in GluR2 C-7 staining in sections from GluR2 K882A KI mice is again attributable to interference of antibody recognition by the K882A point mutation. GluR1 staining in Bergmann glia was comparable between both genotypes.

To assay for GluR2 S880 phosphorylation, we used a previously characterized antibody that was purified to recognize S880 phosphorylation in the presence or absence of a downstream K882A mutation (Chung et al., 2003; Seidenman et al., 2003). Because this phospho-specific antibody crossreacted with the corresponding phosphoserine in the GluR4c AMPA receptor subunit (data not shown), we specifically isolated the GluR2 subunit by immunoprecipitation (IP) after denaturation of brain homogenates in 1% SDS. To our surprise, we found that basal S880 phosphorylation was intact in GluR2 K882A KI mice, with levels similar to that observed in wt littermates (Figure 8A). As a control for specificity, we analyzed samples from GluR2Δ7 KI mice by the exact same IP protocol. In GluR2Δ7 KI mice (which lack the S880 site altogether), basal phosphorylation was

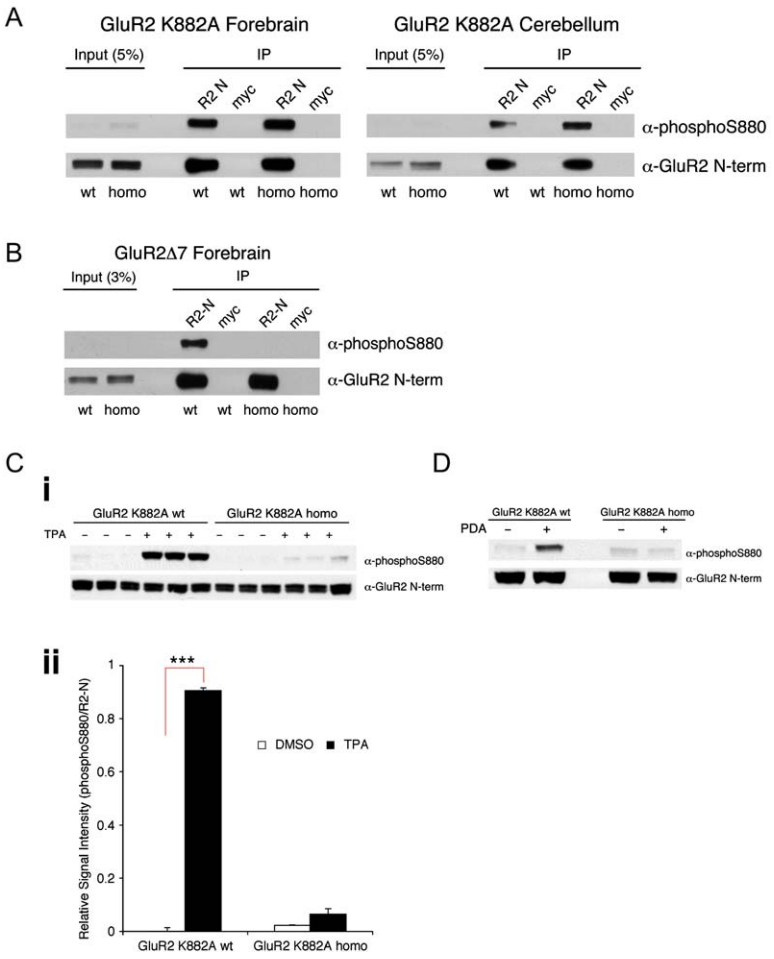

Figure 8. Basal S880 Phosphorylation Is Intact in GluR2 K882A KI Mice, whereas PKC-Mediated S880 Phosphorylation Is Abolished

(A) GluR2 IPs from 3–4 week old forebrains and cerebella show intact S880 phosphorylation in GluR2 K882A KI (homo) mice relative to wt littermates. Samples were denatured in 1% SDS and then diluted in Triton X-100 prior to IP (with α-GluR2-N or α-myc as a control) to disrupt multimeric AMPA receptor complexes. Western blotting was performed with a specially purified phospho-specific S880 antibody (Chung et al., 2003; Seidenman et al., 2003).

(B) Identical IP experiment performed in GluR2Δ7 KI mice and wt littermates as a control.

(C) Phorbol ester stimulation in cortical cultures from GluR2 K882A KI mice and wt littermates. (Ci) 10 day old cortical neurons were treated in triplicate with 200 nM TPA for 20 min (or DMSO as a control), lysed, and analyzed by Western blot with the phospho-specific S880 described in (A). (Cii) S880 phosphorylation signal intensities relative to total GluR2-N signal intensities were quantified for each lane and averaged. Error bars = SEM. Asterisk, $p < 0.05$; triple asterisk, $p << 0.001$.

(D) Phorbol ester stimulation in cerebellar slices from a 4 week old GluR2 K882A KI mouse and its wt littermate. Slices were pooled into two groups per genotype and treated by bath application with either 1 μM PDA for 25 min or DMSO as a control.

completely undetectable (Figure 8B). These data suggest that basal phosphorylation, perhaps mediated by kinases other than PKC, is unaffected in GluR2 K882A KI mice.

To specifically examine PKC-mediated phosphorylation in GluR2 K882A KI mice, we prepared high-density cortical neuron cultures and treated them with either TPA or DMSO as a control. Changes in the levels of S880 phosphorylation were then measured by Western blot with the phospho-specific antibody. Neurons derived from wt mice showed a robust increase in S880 phosphorylation after 20 min of TPA stimulation relative to DMSO-treated controls ($p < 0.001$) (Figure 8C). In contrast, neurons derived from GluR2 K882A KI mice showed no significant increase in S880 phosphorylation after TPA treatment ($p > 0.1$). Basal levels of S880 phosphorylation were not significantly different between wt and GluR2 K882A KI neurons ($p > 0.1$). To confirm these findings in cerebellum, we performed an analogous biochemical experiment with cerebellar tissue slices derived from a 4 week old GluR2 K882A KI mouse and a wt littermate. Slices from each mouse were pooled into two groups containing 10–15 slices each and incubated in perfusion chambers for 25 min with either phorbol ester (PDA, 1 μM) or an equivalent volume of DMSO. In agreement with the results from cortical cultures, a marked increase in S880 phosphorylation was observed for wt slices after PDA treatment (Figure 8D). In slices from GluR2 K882A KI mice, however, S880 phosphorylation levels did not increase beyond basal levels.

We also performed immunoelectron microscopy with a GluR2 N-terminal antibody to analyze the ultrastructural distribution of the mutant receptors (Figure 9). Similar to PICK1 KO and GluR2Δ7 KI mice, GluR2 K882A KI mice showed normal GluR2 labeling at PSDs (10.50 ± 1.50 versus 9.70 ± 1.20 gold particles/μm for wt). However, GluR2 labeling was significantly increased at both extrasynaptic plasma membranes (1.54 ± 0.29 versus 0.76 ± 0.17 gold particles/μm for wt, $p < 0.05$) and intracellularly within spines (34.60 ± 5.60 versus 15.19 ± 2.80 gold particles/μm^2 for wt, $p < 0.001$). Also similar to PICK1 KO and GluR2Δ7 KI mice, GluR2 K882A KI mice showed a concomitant decrease in the degree of intracellular GluR2 labeling in cell bodies and dendrites (6.30 ± 1.13 versus 24.2 ± 3.97 gold particles/μm^2 for wt, $p < 0.001$). These strikingly similar ultrastructural findings in GluR2 K882A KI mice suggest that S880 phosphorylation also regulates GluR2 trafficking in vivo.

Cerebellar LTD Is Absent in GluR2 K882A KI Mice

To check for a deficit in cerebellar LTD, we again performed electrophysiological recordings in both dissociated cultures and acute parasagittal slices from GluR2 K882A KI mice and their wt littermates. LTD was expressed normally in wt cultures (59% ± 8.4% of baseline at t = 40 min, n = 7) (Figure 10A) but was completely

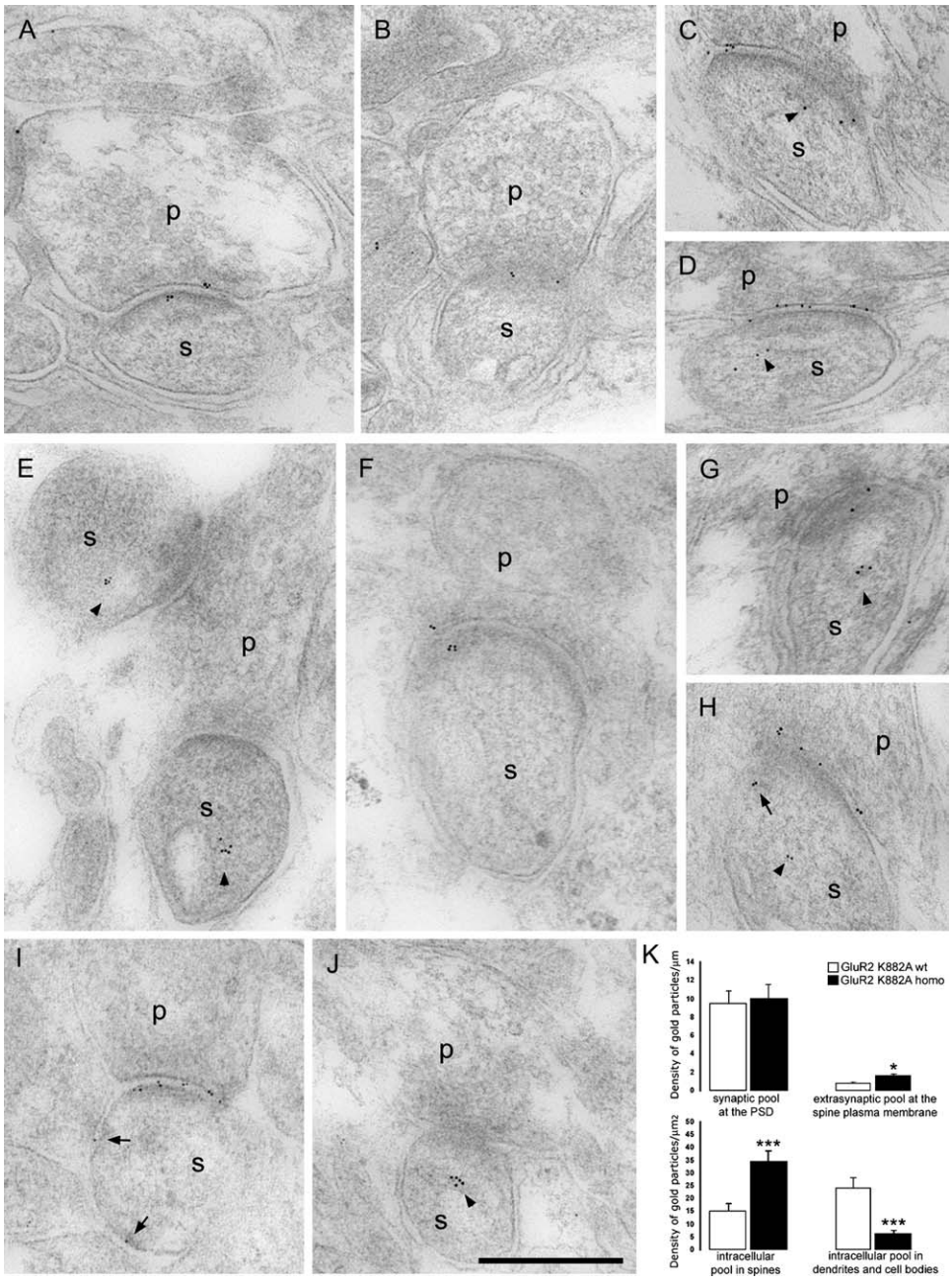

Figure 9. Immunoelectron Microscopy Shows Altered GluR2 Ultrastructural Localization in GluR2 K882A KI Mice

(A–D) Gold particles in wt littermates are again observed predominantly at the PSD with only occasional labeling at the extrasynaptic plasma membrane or intracellularly within spines (arrowheads). (s = Purkinje cell dendritic spine; p = parallel fiber synapses.)

(E–J) PSD labeling in GluR2 K882A KI (homo) mice is comparable to wt littermates, but labeling is increased at the extrasynaptic plasma membrane (arrows) and within the spine intracellular compartment (arrowheads). (s = Purkinje cell dendritic spine; p = parallel fiber synapses.)

(K) Quantitative analysis of immunogold labeling. Histograms show the density/μm of gold particles along the PSD and extrasynaptic spine plasma membrane (upper row) and intracellular density/μm^2 within the spine and in dendrites/cell bodies (lower row). Error bars = SEM. Asterisk, $p < 0.05$; triple asterisk, $p < 0.001$. s = Purkinje cell dendritic spine; p = parallel fiber synapses; scale bar = 0.2 μm.

abolished in those derived from GluR2 K882A KI mice (112% ± 10.7% of baseline at t = 40 min, n = 6). When PDA was used to chemically induce LTD, typical depression of mEPSC amplitudes was observed for wt cultures (from 35 ± 5.6 pA at t = −10 min to 13 ± 6.3 pA at t = 40 min, n = 10) (Figure 10B). Although basal mEPSC amplitudes in GluR2 K882A KI mice were comparable to those of wt littermates, they failed to depress with bath application of PDA (from 33 ± 5.2 pA at t = −10 min to 33 ± 7.5 pA at t = 40 min, n = 10). Acute cerebellar slices from GluR2 K882A KI mice also failed to show LTD (Figure 10C: 101% ± 3.0% of baseline at t = 40 min, n = 6), whereas slices from wt littermates showed normal depression (Figure 10C: 75% ± 2.6% of baseline at t = 40 min, n = 6). Taken together with the biochemical data above, these results demonstrate that PKC-mediated

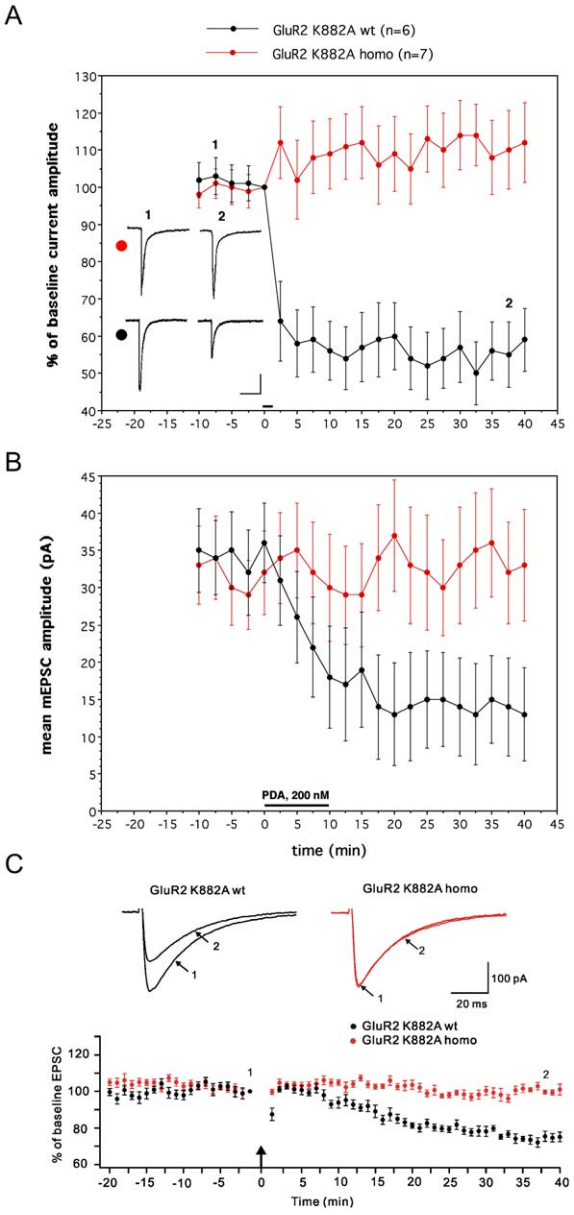

Figure 10. Cerebellar LTD Is Abolished in Cultures and Acute Slices from GluR2 K882A KI Mice

(A) LTD was induced in cultures by six glutamate/depolarization pairings at t = 0 min. Scale bars for representative current traces = 1 s, 30 pA.

(B) An LTD-like effect on mEPSC amplitude was induced in cultures by bath application of PDA as indicated by the horizontal bar. n = 10 cells/group.

(C) Parallel fiber LTD in slices derived from GluR2 K882A mice. n = 6 cells/group. Error bars = SEM for all graphs.

phosphorylation at S880 is essential for cerebellar LTD expression.

Discussion

Deficient Cerebellar LTD in PICK1 KO and GluR2Δ7 KI Mice

In the first part of our analysis, we investigated the roles of PICK1 and the GluR2 C-terminal PDZ ligand in cerebellar LTD by making use of genetically engineered mice lacking the PICK1 protein (PICK1 KO) or the final seven amino acids of the GluR2 intracellular C terminus (GluR2Δ7 KI), respectively. We show here that cerebellar LTD was completely absent in PICK1 KO mice in both dissociated cultures and acute slices. This defect could be rescued by transfection of wt PICK1 in Purkinje cells but not by transfection of a PDZ domain mutant of PICK1 (Staudinger et al., 1997; Xia et al., 1999). Our finding that cerebellar LTD was also abolished in cultures and acute slices from GluR2Δ7 KI mice demonstrates that the PDZ ligand is essential for LTD expression and strongly indicates that the type II PDZ-mediated interaction between PICK1 and GluR2 is necessary for this form of plasticity. It should be noted, however, that because the GluR2Δ7 mutation disrupts GluR2 interaction with both PICK1 and GRIP1/2, our findings with GluR2Δ7 KI mice do not exclude an additionally important role for GRIP1/2 (or other type II PDZ-domain-containing proteins) in cerebellar LTD.

Molecular Roles of PICK1 in Synaptic Function

One key potential role for PICK1 is the facilitation of GluR2 S880 phosphorylation by recruitment of PKCα to GluR2 (Leitges et al., 2004; Lu and Ziff, 2005; Perez et al., 2001). In our studies using neurons derived from PICK1 KO mice, the absence of PICK1 had no effect on TPA-induced increases in GluR2 S880 phosphorylation. Moreover, basal S880 phosphorylation was actually higher in neurons from PICK1 KO mice compared to those from wt littermates. These results suggest that PICK1 is not globally required for PKC-mediated phosphorylation of GluR2 S880. However, we cannot rule out the possibility that PICK1 may be important for regulation of PKC-mediated phosphorylation of GluR2 S880 in response to more physiological stimuli. Nonetheless, our finding that cerebellar LTD was abolished in PICK1 KO mice in response to induction by either phorbol ester or glutamate/depolarization pairing suggests that PICK1 is playing a role in cerebellar LTD that is distinct from the recruitment of PKCα. Our finding that the selective PICK1 K266E/K268E BAR domain mutant failed to rescue LTD from PICK1 KO mice suggests the importance of BAR domain lipid binding in the expression of LTD. Furthermore, it suggests a molecular mechanism by which PICK1 may remodel cellular membranes to facilitate the removal of surface GluR2-containing AMPA receptors during LTD.

Studies in cerebellar stellate cells have suggested an additional role for PICK1 in maintaining a reserve pool of extrasynaptic GluR2-containing receptors for rapid incorporation into the synapse during plasticity (Gardner et al., 2005; Liu and Cull-Candy, 2005). At parallel fiber-stellate cell synapses in the cerebellum, high-frequency stimulation drives a switch in AMPA receptor subtype such that Ca^{2+}-permeable, GluR2-lacking AMPA receptors are replaced by Ca^{2+}-impermeable, GluR2-containing AMPA receptors (Liu and Cull-Candy, 2000). This form of calcium-permeable AMPA receptor plasticity (CARP) is absent in PICK1 KO and GluR2Δ7 KI mice (Gardner et al., 2005). Moreover, PICK1 KO and GluR2Δ7 KI mice appear to have a decrease in the level of GluR2-containing receptors present in the extrasynaptic plasma membrane measured electrophysiologically by

using excised somatic outside-out patches (Gardner et al., 2005). This reduction in extrasynaptic GluR2 content may explain the absence of CARP in PICK1 KO and GluR2Δ7 KI mice through a deficit in the pool of extrasynaptic GluR2-containing AMPA receptors available to mobilize laterally into the synapse. Through a series of rescue studies in GluR2 KO Purkinje cell cultures, we have previously shown that NSF binding is critical for the incorporation of extrasynaptic plasma membrane receptors into the synaptic compartment of Purkinje cells (Steinberg et al., 2004). NSF may act to disrupt PICK1 anchoring of GluR2-containing receptors at extrasynaptic sites, permitting them to diffuse laterally into the synapse to maintain normal basal synaptic transmission and, in the case of stellate cells, to induce a change in synaptic Ca^{2+} permeability upon high-frequency stimulation.

Despite a complete impairment in CARP, cerebellar stellate cells in PICK1 KO and GluR2Δ7 KI mice appear to have normal basal synaptic transmission (Gardner et al., 2005). This is consistent with our present findings of normal mEPSC amplitudes in Purkinje cells derived from PICK1 KO and GluR2Δ7 KI mice despite the complete absence of cerebellar LTD. It is also consistent with the results of studies involving peptide perfusion into Purkinje cells, in which GluR2 C-terminal peptides designed to interfere with PICK1-GluR2 PDZ-dependent interactions had no effect on AMPA-mediated mEPSCs but produced a large attenuation of LTD (Xia et al., 2000). Our immunoelectron microscopic analysis showing an equivalent degree of GluR2 labeling at the PSD for PICK1 KO and GluR2Δ7 KI mice and their wt littermates supports the data on mEPSC amplitudes. Altogether, these results suggest that PICK1 is not critical for maintaining basal synaptic levels of GluR2 or that a compensatory mechanism maintains tight regulation over the level of synaptic AMPA receptors in vivo.

Interestingly, we observed a significant increase in the degree of both extrasynaptic plasma membrane and intracellular GluR2 immunogold labeling within the spines of PICK1 KO and GluR2Δ7 KI mice. The increase in extrasynaptic plasma membrane labeling appears to be at odds with the finding of reduced GluR2-containing receptors (and therefore lower GluR2 content) in cerebellar stellate cells from PICK1 KO and GluR2Δ7 KI mice using excised somatic outside-out patches (Gardner et al., 2005). It should be noted, however, that we observed increases in GluR2 immunogold labeling only at the extrasynaptic plasma membrane of spines and could not detect any changes in labeling at dendritic or somatic plasma membranes because of the relatively low density of AMPA receptors at these locations. The extrasynaptic plasma membrane in spines may differ from the perisynaptic plasma membrane of dendrites and from the plasma membrane of cell bodies where the excised outside-out patches were isolated (Gardner et al., 2005). In general, our results indicate a redistribution of GluR2 from cell bodies and dendrites to extrasynaptic regions in spines in PICK1 KO and GluR2Δ7 KI as well as GluR2 K882A KI mice. We believe that this strikingly similar accumulation of GluR2 in the spines of all three mutants reflects aberrant receptor trafficking that contributes to the blockade of plasticity. Identification of the specific trafficking defects will require future imaging studies in cerebellar preparations from the mutant mice.

Intact Basal, but Impaired PKC-Mediated, Phosphorylation and Deficient Cerebellar LTD in GluR2 K882A KI Mice

Our findings indicate that GluR2 K882A KI mice with a disruption in the C-terminal PKC consensus motif have normal levels of basal S880 phosphorylation compared to wt littermates in both forebrain and cerebellum. In contrast, PKC-mediated phosphorylation of S880 in response to phorbol ester stimulation is completely abolished in samples from both brain regions. Previous studies have shown that PKCα is the critical kinase in Purkinje cells mediating expression of LTD (Leitges et al., 2004). Our results demonstrate that S880 is a key substrate for PKCα and is absolutely required for expression of cerebellar LTD and support a model (Chung et al., 2000, 2003; Matsuda et al., 1999) in which S880 phosphorylation disrupts GRIP1/2 binding and promotes PICK1 binding and AMPA receptor endocytosis.

LTD at the parallel fiber-Purkinje cell synapse in the cerebellum has long been hypothesized to form a major portion of the engram for certain types of motor learning (Bear and Linden, 2000; Boyden et al., 2004; Linden, 2003). Previous studies in transgenic mice lacking cerebellar LTD have associated this deficit with altered performance in behavioral paradigms such as associative eyelid conditioning (Aiba et al., 1994; Kishimoto et al., 2001; Koekkoek et al., 2003; Shibuki et al., 1996) and adaptation of the vestibulo-ocular reflex (De Zeeuw et al., 1998; Feil et al., 2003). Conclusive evidence linking LTD to behavior awaits further experimentation because interpretation of a number of previous studies is confounded by the presence of generalized motor disturbances and/or abnormal cerebellar development in the mutant mice (Aiba et al., 1994; Kashiwabuchi et al., 1995). Moreover, many mouse models have involved complete ablation or inhibition of kinases such as PKC (De Zeeuw et al., 1998) and cGMP-dependent protein kinase I (Feil et al., 2003) or receptors such as mGluR1 (Aiba et al., 1994) and the orphan GluRδ2 (Kashiwabuchi et al., 1995). Because these kinases and receptors have multiple targets and multiple effects, respectively, these relatively nonspecific manipulations make it difficult to link behavioral deficits with the absence of cerebellar LTD.

The GluR2 K882A KI mouse may represent an important tool for behavioral analysis. First, cerebellar morphology and development appears normal in GluR2 K882A KI mice. Second, basal synaptic transmission appears normal in Purkinje cells of GluR2 K882A KI mice. Third, binding of GluR2 to PDZ domain-containing proteins is unaltered (Chung et al., 2003; Seidenman et al., 2003) because of mutation at a noncritical residue for PDZ binding (Songyang et al., 1997). Fourth, S880 phosphorylation is not disrupted basally but rather only in response to signals that activate PKC. Fifth, cerebellar LTD is completely abolished in both cultures and acute slices in a fashion that is independent of side effects on signals upstream of PKCα activation. Thus, future studies using the GluR2 K882A KI mice may help to more clearly delineate the role of cerebellar LTD in cerebellar motor learning.

Experimental Procedures

Biochemical Analysis of Mutant Mice

For Western blot detection of AMPA receptor levels in each of the three mutant mouse lines, hippocampi and cerebella were dissected from 3–4 week old (1 month old) or 3 month old mice (KO/KI and wt littermates) and sonicated to homogeneity in 320 mM sucrose, 10 mM Tris (pH 7.4), 5 mM EDTA, Complete protease inhibitor cocktail (Roche), 1 μM microcystin-LR, and 1 mM sodium orthovanadate (Buffer H). Protein samples were denatured in SDS buffer and loaded (10 μg/well) onto 7.5% polyacrylamide gels. Separated proteins were transferred onto PVDF membranes (Millipore) and blotted with homemade primary antibodies as described in the text or commercially available anti-tubulin (Sigma).

For IP experiments, P2 fractions were first prepared from 3–4 week old mice (KO/KI and wt littermates). Briefly, forebrains and cerebella were dissected, homogenized in Buffer H with 20 strokes with a Glas-Col homogenizer, and cleared by centrifugation at 700 × g for 10 min. Supernatants were then respun at 37,000 × g for 16 min to obtain the P2 pellet. P2 fractions were resuspended in 10 mM Tris (pH 7.4), 5 mM EDTA, Complete protease inhibitor cocktail (Roche), 1 μM microcystin-LR, and 1 mM sodium orthovanadate (Buffer TE). For IP, 500 μg P2 aliquots were diluted to 2 mg/ml in Buffer TE, sonicated briefly, then extracted for 30 min at 4ºC by the addition of SDS to 1% final concentration. The SDS was then diluted to 0.2% by the addition of Buffer TE containing Triton X-100, NaCl, and DTT for final concentrations of 1%, 0.25 M, and 10 mM, respectively, and further incubated for 30 min at 4ºC. For the GluR2L/GluR2/3/4c immunodepletion experiment, P2 aliquots were instead extracted in Buffer TE containing 1.5% Triton X-100. Extracted P2 samples were precleared for 1 hr prior to incubation with antibody-coupled Protein A-Sepharose beads for 3 hr. After incubation, immunoprecipitates were washed extensively, boiled, and loaded onto 7.5% gels.

For phorbol ester stimulation in cultured neurons, high-density cortical cultures were prepared from P0–P1 pups according to methods previously described for the rat (Rumbaugh et al., 2003). Cortices from two to three KO/KI pups and their wt littermates were pooled separately according to genotype, dissociated, and plated in 6-well dishes at a density of 100,000 cells/cm^2. On day in vitro (div) 10, neurons were treated in duplicate or triplicate with 200 nM TPA (Calbiochem) or an equivalent volume of DMSO for 20 min at 37ºC. Cultures were placed on ice, washed once with ice-cold Tris-buffered saline, and solubilized in Buffer TE containing 1.5% Triton X-100 for 30 min at 4ºC. Samples were then centrifuged at 16,100 × g and loaded (12.5 μg/well) onto 7.5% gels. Quantitative analysis was performed with NIH ImageJ 1.34s freeware. Two-tailed t tests (assuming equal variance) were used for statistical comparison.

For phorbol ester stimulation in cerebellar slices, 200 μm thick sagittal slices of whole cerebellum were prepared from a 4 week old GluR2 K882A KI mouse and its wt littermate with a vibrating tissue slicer (Leica) and ice-cold standard artificial cerebrospinal fluid (ACSF) containing (in mM) 124 NaCl, 2.5 KCl, 1.3 $MgCl_2$, 2.5 $CaCl_2$, 1 NaH_2PO_4, 26.2 $NaHCO_3$, and 20 glucose bubbled with 95% O_2/5% CO_2 (pH 7.4). Slices from each mouse were then divided into two approximately equal groups (10–15 slices each) and incubated in perfusion chambers with ACSF containing 1 μM PDA (Sigma) or an equivalent volume of DMSO for 25 min at room temperature (RT). Slices were then transferred into tubes containing Buffer TE, sonicated to homogeneity, and loaded (25 μg/well) onto 7.5% gels.

Immunoelectron Microscopy

For electron microscopy, cerebellar regions were dissected, sectioned with a Vibratome, and processed for freeze-substitution and low-temperature embedding as previously described (Matsui et al., 2005). Postembedding immunogold labeling of the GluR2 AMPA receptor subunit was performed with a monoclonal antibody to the N terminus (1:300; Chemicon) following a similar protocol to that detailed previously (Matsui et al., 2005; Rubio and Soto, 2001). Primary antibody was labeled with 5 nm colloidal gold-coupled secondary antibodies (Amersham). Control experiments were performed by omitting the primary antibody. Electron micrographs were taken at 34,300× magnification with a Philips 300M transmission electron microscope and scanned at a resolution of 1600 dpi with an Epson Expression 1680 scanner. Image processing was performed with Adobe Photoshop with only the brightness and contrast commands to enhance gold particles.

Identification of parallel fiber synapses on Purkinje cells was based on defined criteria (Matsui et al., 2005; Rubio and Soto, 2001). The distribution and relative density of GluR2 immunolabeling was determined for 60 parallel fiber-Purkinje cell synapses for each of the three pairs of wt and KO/KI mice analyzed. The linear density of gold particles at the PSD (n = 60 profiles) and at the extrasynaptic plasma membrane (n = 60 profiles) was computed with NIH Scion Image by dividing the number of gold particles in a PSD profile by the membrane length of that profile. The density of intracellular labeling in the spine (n = 60 profiles) or intracellular labeling within cell bodies and dendrites (n = 15 profiles, each with an average area of 3–5 μm^2) was calculated by dividing the number of gold particles in a profile by the area of that profile. The average linear density and density per area were computed across all profiles. Two-tailed t tests (assuming unequal variance) were used for statistical comparison.

Cerebellar Culture Preparation

For GluR2Δ7 and GluR2 K882A mutant mouse lines, wt and homozygous mice were mated separately. Cerebella from E18 pups were then dissected and pooled into two separate groups according to genotype. Because homozygous mating was not productive in PICK1 mutant mice, heterozygotes were intercrossed. Tail samples from P0 pups were digested with proteinase K and genotyped by PCR immediately prior to culture. Cerebellar dissection, dissociation, plating, and gene gun-mediated transfection were performed as previously described (Chung et al., 2003; Linden, 2001). Cultures were generally transfected on div 6 and recordings were begun 20–50 hr later.

Electrophysiology

Electrophysiology in cultures was performed as previously described (Chung et al., 2003; Steinberg et al., 2004). For slice recordings, sagittal (250 μm thick) slices of the cerebellar vermis were first prepared from P20–P25 mice with a vibrating tissue slicer and ice-cold standard ACSF. Slices were recovered for 30 min in a warm chamber at 37ºC and further recovered for 1 hr at RT. The slices were placed in a submerged chamber that was perfused at a flow rate of 2 ml/min with room temperature ACSF and 20 μM gabazine to block $GABA_A$ receptors. Visualized whole-cell patch-clamp recording was performed with a Zeiss Axioskop 2FS equipped with Dodt gradient contrast illumination. The electrodes for Purkinje cell recording (2–4 MΩ) were filled with a solution containing (in mM) 135 Cs-methanesulfonate, 10 CsCl, 10 HEPES, 0.2 EGTA, 4 Na_2-ATP, and 0.4 Na-GTP (pH 7.2). Cells were voltage clamped at −70 mV. The currents were filtered at 2 kHz and digitized at 10 kHz. For parallel fiber stimulation, standard patch pipettes filled with ACSF were placed in the molecular layer and test stimulation was given by using paired pulses (80 ms interval) at a frequency of 0.1 Hz with 100–150 μA pulses (100 μs duration). Stimulus strength was adjusted so that the first EPSC did not exceed 400 pA. To induce LTD, we stimulated parallel fibers with a burst of five pulses at 100 Hz, which was accompanied by 100 ms long depolarization of the Purkinje cell to 0 mV, repeated 30 times with an interburst interval of 2 s. A total of 30 trains were applied at 2 s intervals. The experimenter was blind to the mouse genotype until after data analysis.

PICK1 cDNA Mutagenesis and Lipid Binding Assays

PICK1 point mutant constructs were created by PCR mutagenesis with complete sequence verification. Lipid binding assays were performed according to a previously detailed method (Peter et al., 2004). Briefly, equimolar amounts of purified PICK1 fusion protein (wt and mutants) were incubated with brain lipid extracts (Folch fraction I; Sigma) for 15 min at 37ºC and then centrifuged at 140,000 × g for 15 min at 4ºC. Supernatants were separated and pellets resuspended in equal volumes of buffer before SDS-PAGE analysis and Coomassie blue staining. Quantification was performed by densitometric analysis as described above (n = 6 experiments per construct).

Supplemental Data

The Supplemental Data for this article can be found online at http://www.neuron.org/cgi/content/full/49/6/845/DC1/.

Acknowledgments

We thank R. Bock for superior technical assistance with cerebellar culture preparation, C. Yu for assistance with mouse-line maintenance and histologic analysis, R. Johnson for technical assistance with cDNA mutagenesis, M. Coulter for antibody preparation, N. Ramanan for assistance with Golgi staining and microscope image acquisition, and D.T. Lin for assistance with image processing and quantification. This work was supported by research grants from the National Institutes of Health NS 36715, the Robert Packard Center for ALS Research, and the Muscular Dystrophy Association's Wings Over Wall Street (to R.L.H); by PHS MH51106 and the Develbiss Fund (to D.J.L.); and by Research Grants Council of Hong Kong (to J.X.). Under a licensing agreement between Upstate Group, Inc., and The Johns Hopkins University, R.L.H. is entitled to a share of royalties received by the University on sales of products described in this article. R.L.H. is a paid consultant to Upstate Group, Inc. The terms of this arrangement are being managed by The Johns Hopkins University in accordance with its conflict-of-interest policies.

Received: October 25, 2005
Revised: February 9, 2006
Accepted: February 28, 2006
Published: March 15, 2006

References

Aiba, A., Kano, M., Chen, C., Stanton, M.E., Fox, G.D., Herrup, K., Zwingman, T.A., and Tonegawa, S. (1994). Deficient cerebellar long-term depression and impaired motor learning in mGluR1 mutant mice. Cell *79*, 377–388.

Baude, A., Molnar, E., Latawiec, D., McIlhinney, R.A., and Somogyi, P. (1994). Synaptic and nonsynaptic localization of the GluR1 subunit of the AMPA-type excitatory amino acid receptor in the rat cerebellum. J. Neurosci. *14*, 2830–2843.

Bear, M.F., and Linden, D.J. (2000). The mechanisms and meaning of long-term synaptic depression in the mammalian brain. In The Synapse, W.M. Cowan and K. Davies, eds. (Baltimore, MD: Johns Hopkins University Press), pp. 455–517.

Blanpied, T.A., Scott, D.B., and Ehlers, M.D. (2002). Dynamics and regulation of clathrin coats at specialized endocytic zones of dendrites and spines. Neuron *36*, 435–449.

Boyden, E.S., Katoh, A., and Raymond, J.L. (2004). Cerebellum-dependent learning: the role of multiple plasticity mechanisms. Annu. Rev. Neurosci. *27*, 581–609.

Chung, H.J., Xia, J., Scannevin, R.H., Zhang, X., and Huganir, R.L. (2000). Phosphorylation of the AMPA receptor subunit GluR2 differentially regulates its interaction with PDZ domain-containing proteins. J. Neurosci. *20*, 7258–7267.

Chung, H.J., Steinberg, J.P., Huganir, R.L., and Linden, D.J. (2003). Requirement of AMPA receptor GluR2 phosphorylation for cerebellar long-term depression. Science *300*, 1751–1755.

De Zeeuw, C.I., Hansel, C., Bian, F., Koekkoek, S.K., van Alphen, A.M., Linden, D.J., and Oberdick, J. (1998). Expression of a protein kinase C inhibitor in Purkinje cells blocks cerebellar LTD and adaptation of the vestibulo-ocular reflex. Neuron *20*, 495–508.

Dev, K.K., Nishimune, A., Henley, J.M., and Nakanishi, S. (1999). The protein kinase C alpha binding protein PICK1 interacts with short but not long form alternative splice variants of AMPA receptor subunits. Neuropharmacology *38*, 635–644.

Feil, R., Hartmann, J., Luo, C., Wolfsgruber, W., Schilling, K., Feil, S., Barski, J.J., Meyer, M., Konnerth, A., De Zeeuw, C.I., and Hofmann, F. (2003). Impairment of LTD and cerebellar learning by Purkinje cell-specific ablation of cGMP-dependent protein kinase I. J. Cell Biol. *163*, 295–302.

Gardner, S.M., Takamiya, K., Xia, J., Suh, J.G., Johnson, R., Yu, S., and Huganir, R.L. (2005). Calcium-permeable AMPA receptor plasticity is mediated by subunit-specific interactions with PICK1 and NSF. Neuron *45*, 903–915.

Habermann, B. (2004). The BAR-domain family of proteins: a case of bending and binding? EMBO Rep. *5*, 250–255.

Ito, M. (2002). The molecular organization of cerebellar long-term depression. Nat. Rev. Neurosci. *3*, 896–902.

Kashiwabuchi, N., Ikeda, K., Araki, K., Hirano, T., Shibuki, K., Takayama, C., Inoue, Y., Kutsuwada, T., Yagi, T., Kang, Y., et al. (1995). Impairment of motor coordination, Purkinje cell synapse formation, and cerebellar long-term depression in GluR delta 2 mutant mice. Cell *81*, 245–252.

Kemp, B.E., and Pearson, R.B. (1990). Protein kinase recognition sequence motifs. Trends Biochem. Sci. *15*, 342–346.

Kishimoto, Y., Kawahara, S., Suzuki, M., Mori, H., Mishina, M., and Kirino, Y. (2001). Classical eyeblink conditioning in glutamate receptor subunit delta 2 mutant mice is impaired in the delay paradigm but not in the trace paradigm. Eur. J. Neurosci. *13*, 1249–1253.

Koekkoek, S.K., Hulscher, H.C., Dortland, B.R., Hensbroek, R.A., Elgersma, Y., Ruigrok, T.J., and De Zeeuw, C.I. (2003). Cerebellar LTD and learning-dependent timing of conditioned eyelid responses. Science *301*, 1736–1739.

Leitges, M., Kovac, J., Plomann, M., and Linden, D.J. (2004). A unique PDZ ligand in PKCalpha confers induction of cerebellar long-term synaptic depression. Neuron *44*, 585–594.

Linden, D.J. (2001). The expression of cerebellar LTD in culture is not associated with changes in AMPA-receptor kinetics, agonist affinity, or unitary conductance. Proc. Natl. Acad. Sci. USA *98*, 14066–14071.

Linden, D.J. (2003). Neuroscience. From molecules to memory in the cerebellum. Science *301*, 1682–1685.

Linden, D.J., and Connor, J.A. (1991). Participation of postsynaptic PKC in cerebellar long-term depression in culture. Science *254*, 1656–1659.

Liu, S.Q., and Cull-Candy, S.G. (2000). Synaptic activity at calcium-permeable AMPA receptors induces a switch in receptor subtype. Nature *405*, 454–458.

Liu, S.J., and Cull-Candy, S.G. (2005). Subunit interaction with PICK and GRIP controls Ca^{2+} permeability of AMPARs at cerebellar synapses. Nat. Neurosci. *8*, 768–775.

Lu, W., and Ziff, E.B. (2005). PICK1 interacts with ABP/GRIP to regulate AMPA receptor trafficking. Neuron *47*, 407–421.

Matsuda, S., Mikawa, S., and Hirai, H. (1999). Phosphorylation of serine-880 in GluR2 by protein kinase C prevents its C terminus from binding with glutamate receptor-interacting protein. J. Neurochem. *73*, 1765–1768.

Matsuda, S., Launey, T., Mikawa, S., and Hirai, H. (2000). Disruption of AMPA receptor GluR2 clusters following long-term depression induction in cerebellar Purkinje neurons. EMBO J. *19*, 2765–2774.

Matsui, K., Jahr, C.E., and Rubio, M.E. (2005). High-concentration rapid transients of glutamate mediate neural-glial communication via ectopic release. J. Neurosci. *25*, 7538–7547.

Perez, J.L., Khatri, L., Chang, C., Srivastava, S., Osten, P., and Ziff, E.B. (2001). PICK1 targets activated protein kinase Calpha to AMPA receptor clusters in spines of hippocampal neurons and reduces surface levels of the AMPA-type glutamate receptor subunit 2. J. Neurosci. *21*, 5417–5428.

Peter, B.J., Kent, H.M., Mills, I.G., Vallis, Y., Butler, P.J., Evans, P.R., and McMahon, H.T. (2004). BAR domains as sensors of membrane curvature: the amphiphysin BAR structure. Science *303*, 495–499.

Racz, B., Blanpied, T.A., Ehlers, M.D., and Weinberg, R.J. (2004). Lateral organization of endocytic machinery in dendritic spines. Nat. Neurosci. *7*, 917–918.

Rubio, M.E., and Soto, F. (2001). Distinct Localization of P2X receptors at excitatory postsynaptic specializations. J. Neurosci. *21*, 641–653.

Rumbaugh, G., Sia, G.M., Garner, C.C., and Huganir, R.L. (2003). Synapse-associated protein-97 isoform-specific regulation of surface AMPA receptors and synaptic function in cultured neurons. J. Neurosci. *23*, 4567–4576.

Seidenman, K.J., Steinberg, J.P., Huganir, R., and Malinow, R. (2003). Glutamate receptor subunit 2 Serine 880 phosphorylation modulates synaptic transmission and mediates plasticity in CA1 pyramidal cells. J. Neurosci. *23*, 9220–9228.

Shibuki, K., Gomi, H., Chen, L., Bao, S., Kim, J.J., Wakatsuki, H., Fujisaki, T., Fujimoto, K., Katoh, A., Ikeda, T., et al. (1996). Deficient cerebellar long-term depression, impaired eyeblink conditioning, and normal motor coordination in GFAP mutant mice. Neuron *16*, 587–599.

Songyang, Z., Fanning, A.S., Fu, C., Xu, J., Marfatia, S.M., Chishti, A.H., Crompton, A., Chan, A.C., Anderson, J.M., and Cantley, L.C. (1997). Recognition of unique carboxyl-terminal motifs by distinct PDZ domains. Science *275*, 73–77.

Staudinger, J., Zhou, J., Burgess, R., Elledge, S.J., and Olson, E.N. (1995). PICK1: a perinuclear binding protein and substrate for protein kinase C isolated by the yeast two-hybrid system. J. Cell Biol. *128*, 263–271.

Staudinger, J., Lu, J., and Olson, E.N. (1997). Specific interaction of the PDZ domain protein PICK1 with the COOH terminus of protein kinase C-alpha. J. Biol. Chem. *272*, 32019–32024.

Steinberg, J.P., Huganir, R.L., and Linden, D.J. (2004). N-ethylmaleimide-sensitive factor is required for the synaptic incorporation and removal of AMPA receptors during cerebellar long-term depression. Proc. Natl. Acad. Sci. USA *101*, 18212–18216.

Tarricone, C., Xiao, B., Justin, N., Walker, P.A., Rittinger, K., Gamblin, S.J., and Smerdon, S.J. (2001). The structural basis of Arfaptin-mediated cross-talk between Rac and Arf signalling pathways. Nature *411*, 215–219.

Wang, Y.T., and Linden, D.J. (2000). Expression of cerebellar long-term depression requires postsynaptic clathrin-mediated endocytosis. Neuron *25*, 635–647.

Xia, J., Zhang, X., Staudinger, J., and Huganir, R.L. (1999). Clustering of AMPA receptors by the synaptic PDZ domain-containing protein PICK1. Neuron *22*, 179–187.

Xia, J., Chung, H.J., Wihler, C., Huganir, R.L., and Linden, D.J. (2000). Cerebellar long-term depression requires PKC-regulated interactions between GluR2/3 and PDZ domain-containing proteins. Neuron *28*, 499–510.